DOE/MC/30012 -- 5178
(DE96004455)

Advanced Sulfur Control Concepts for Hot Gas Desulfurization Technology

Quarterly Report
October - December 1995

January 1996

Work Performed Under Contract No.: DE-AC21-94MC30012

For
U.S. Department of Energy
Office of Fossil Energy
Morgantown Energy Technology Center
Morgantown, West Virginia

By
Louisiana State University
Baton Rouge, Louisiana 70803

DISCLAIMER

DOE/MC/30012 -- 5178
(DE96004455)
Distribution Category UC-106

Advanced Sulfur Control Concepts for Hot Gas Desulfurization Technology

Quarterly Report
October - December 1995

Work Performed Under Contract No.: DE-AC21-94MC30012

For
U.S. Department of Energy
Office of Fossil Energy
Morgantown Energy Technology Center
P.O. Box 880
Morgantown, West Virginia 26507-0880

By
Louisiana State University
Department of Chemical Engineering
Baton Rouge, Louisiana 70803

January 1996

EXECUTIVE SUMMARY

In the area of gas analysis, most of the attention during the past quarter was devoted to gaining an understanding of the operation of the Antek total sulfur analyzer, and making appropriate modifications in the unit. The primary problem is that the resistance of the capillary flow restrictor is not large enough, and the amount of sulfur which reaches the UV-analyzer results in the analyzer becoming saturated. We have added a N_2 diluent flow downstream of the pyrotube tube which, we believe, will permit the unit to be operated at pressures to about 50 psig. Use of larger diluent flow rates to permit higher pressure operation is not feasible since larger diluent rates increase the back pressure on the quartz pyrotube (which operates at 1050°C) to unsafe levels. In the meantime, Antek is studying the redesign of the capillary flow restrictor to provide larger flow resistance.

Studies on the regeneration of FeS in the atmospheric pressure reactor were almost completed during the quarter. Only a series of multicycle sulfidation-regeneration tests remains. The effects of reactive gas mol fraction and temperature have been examined using both O_2/N_2 and H_2O/N_2 atmospheres. The initial rate of regeneration was found to be a weak function of temperature and first-order in both O_2 and H_2O concentration. In a test series in which the reactive gas contained both O_2 and H_2O, the experimental initial rate was effectively equal to the sum of the individual initial rates, suggesting that the two reactions proceed independently of one another. Detailed correlation and statistical analysis of the data is currently being done.

Principal effort during the quarter using the high pressure electrobalance was devoted to studying the regeneration of FeS in a H_2O/N_2 atmosphere. Experimental difficulties involving steam condensation in high pressure tests slowed progress. The steam diffused to cold spots in the hangdown tube where it condensed. Drops would build-up and subsequently fall into the heated zone. There, the drops would vaporize almost instantaneously and create a shock wave which altered the results, and, in some instances, had sufficient force to displace sample from the sample pan. This problem was resolved by heat tracing those portions of the hang-down tube where condensation occurred. The effects of temperature and reactive gas mol fraction were qualitatively similar to those observed in the atmospheric pressure tests. The temperature effect was small and the initial rate was first order in both O_2 and H_2O. The initial rate increased with pressure between 1 and 5 atm, and subsequently decreased between 5 and 15 atm.

GAS ANALYSIS

At the end of the previous quarter both the Antek total sulfur analyzer and the gas chromatograph had been delivered and installed. The GC appeared to be working properly but problems existed, and still exist, with the Antek analyzer. Much of the effort during the quarter was directed toward resolving these problems. Progress, although slow, has been made and we believe that the system is almost operable at reactor pressure equal to or less than 50 psig.

The flow rate of reactor product through the Antek analyzer is determined strictly by the pressure upstream of the capillary flow restrictor. The resistance of the current quartz restrictor

is too small, with the result that sulfur flow rates saturate the UV-analyzer. Calibration curves of instrument response versus percent sulfur always contained a maximum so that the same instrument reading corresponded to two different concentrations. The point of the maximum shifted to higher sulfur concentrations as the feed pressure was decreased.

When the normalized results of several calibration tests at different pressures were plotted versus the mol fraction SO_2 to the detector (see Figure 1), we found that all of the curves effectively collapsed into a single curve having a maximum at about 0.03 mol fraction SO_2. The y-axis in Figure 1 was obtained by dividing the Antek response at given conditions to the maximum Antek response for the particular test. In tests 1, 3, 4, and 5 in Figure 1, the only variable was inlet pressure, which, as previously stated, produced a variation in flow rate. In analyzing the data from tests 1 through 5, it became obvious that extending the analytical range to higher sulfur concentrations could be accomplished only be reducing the sample flow at a given inlet pressure or by diluting the gas between the pyrotube and the UV-detector. Antek is continuing to work on the design of a new capillary flow restrictor to provide increased flow resistance and decreased flow rate.

In the interim, we have added a N_2 diluent between the pyrotube and the detector as shown in Figure 2. Diluent was added in tests 6 and 7, and, as shown in Figure 1, the results are effectively identical to results from tests not using the diluent. In test 6, the inlet pressure was 180 psig which produced a sample flow rate of 180 sccm (Q_1). 437 sccm of O_2 was added to the pyrotube (Q_2) and 2800 sccm of N_2 diluent (Q_3) was added downstream of the pyrotube. The operating pressure and O_2 addition rate were the same as in test 1, and, as shown in Figure 1, the results in terms of normalized instrument response versus percent SO_2 were practically the same. The addition of 2800 sccm N_2 diluted the sulfur concentration to the detector by a factor of 5.53 (3417/617), and shifted the peak in the response curve based on inlet H_2S concentration from about 1.1% H_2S without diluent to 4.3% H_2S as shown in Figure 3. However, this high rate of N_2 dilution increased the back pressure on the pyrotube to about 4.5 psig, which is too large for normal operation.

Calibration test 7 used 50 psig inlet pressure which produced a sample flow of 25 sccm. Coupled with 437 sccm of O_2 and 371 sccm of N_2 diluent, the dilution factor was 1.8. Figure 4 compares the calibration curve for test 7 on the basis of H_2S percent with the curve from test 4 without N_2 dilution, but otherwise at the same conditions. The 1.8 dilution factor shifted the peak in the curve from about 3% H_2S to about 9% H_2S. Back pressure in this case was not excessive and the test 7 results form the basis for our current belief that diluent addition may make the Antek unit satisfactory for reactor operating pressures up to about 50 psig. The unnormalized test 7 results were fit to a quadratic equation to give

$$y = 1749\,x - 9.35\,x^2 + 13$$

where y is the Antek instrument response and x is the mol percent H_2S in the feed gas.

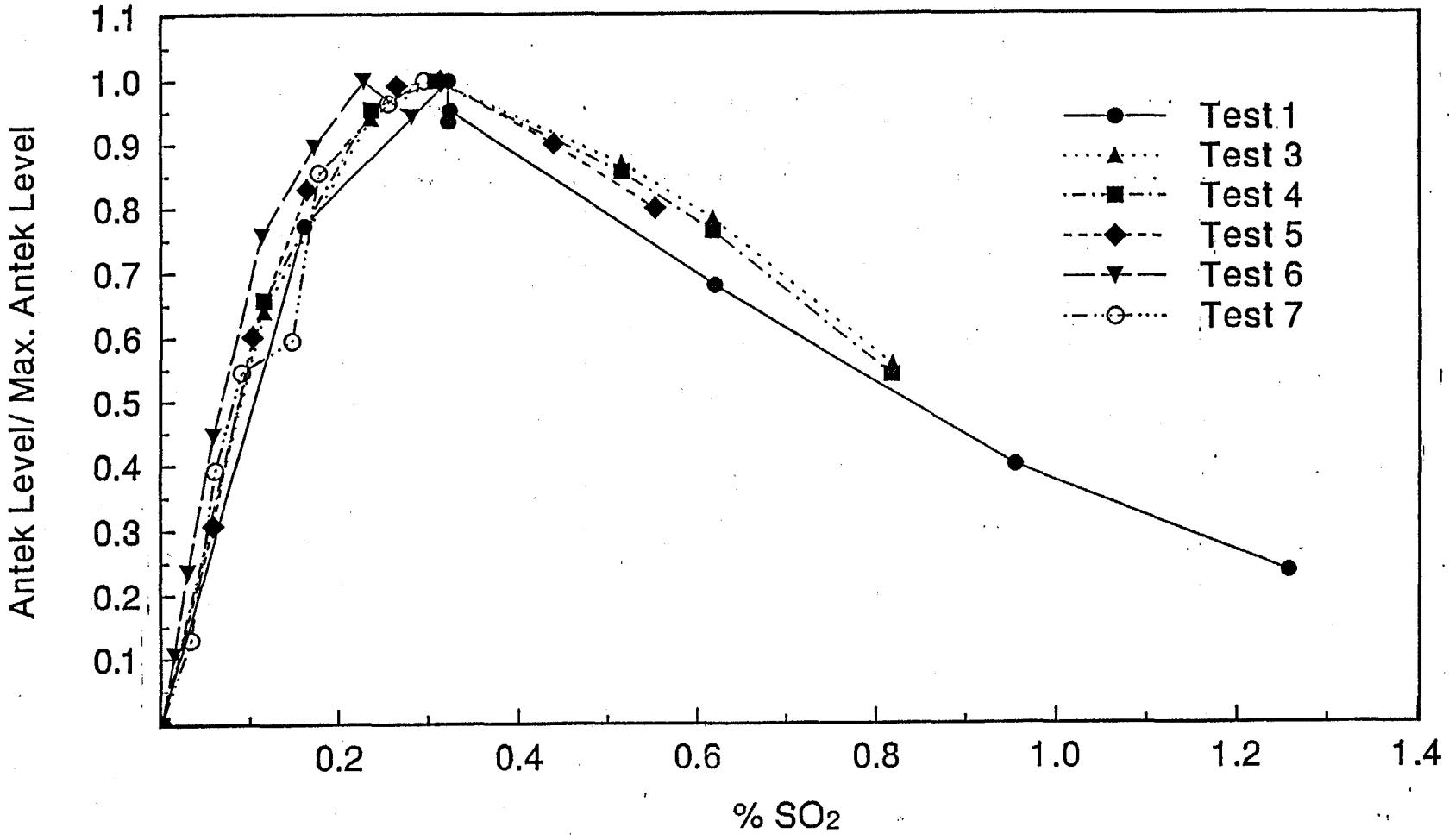

Figure 1. Antek Calibration Curves Based Upon the Concentration of SO_2 to the Detector

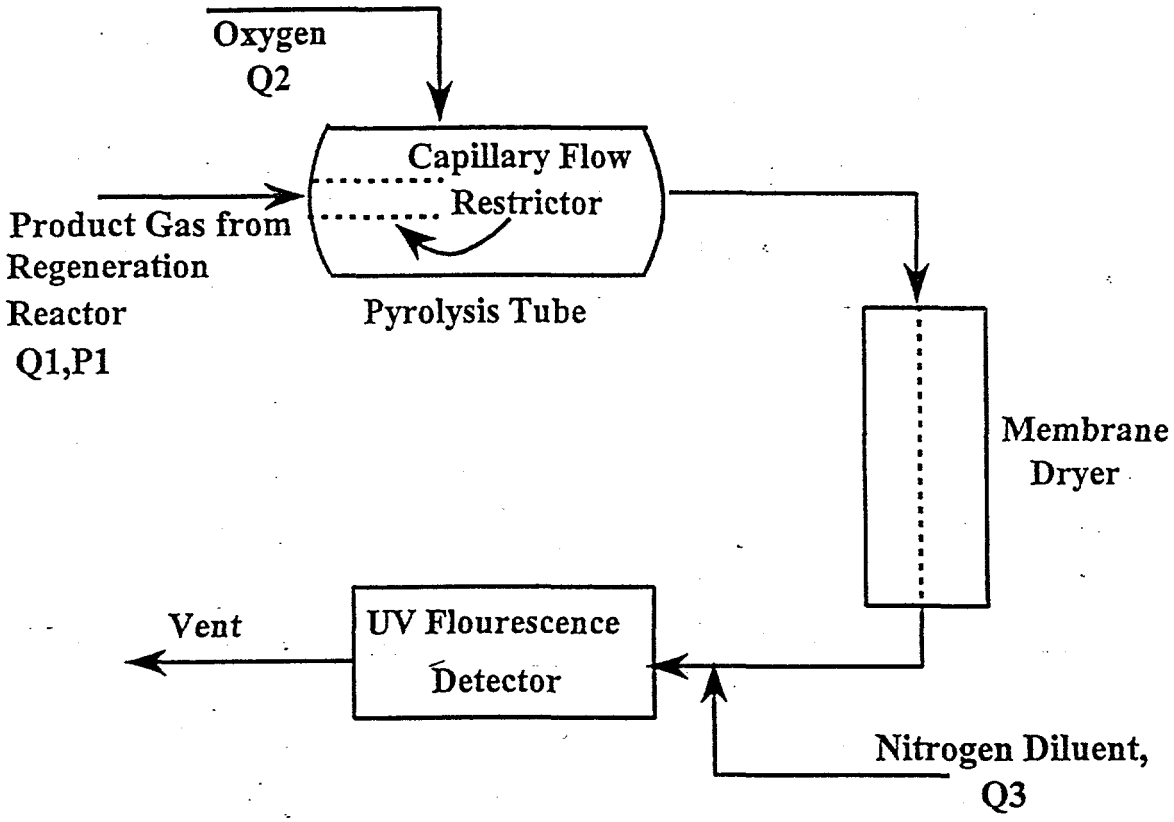

Figure 2. Simplified Flow Diagram of the Antek Total Sulfur Analyzer After Diluting The Pyrotube Product With Nitrogen

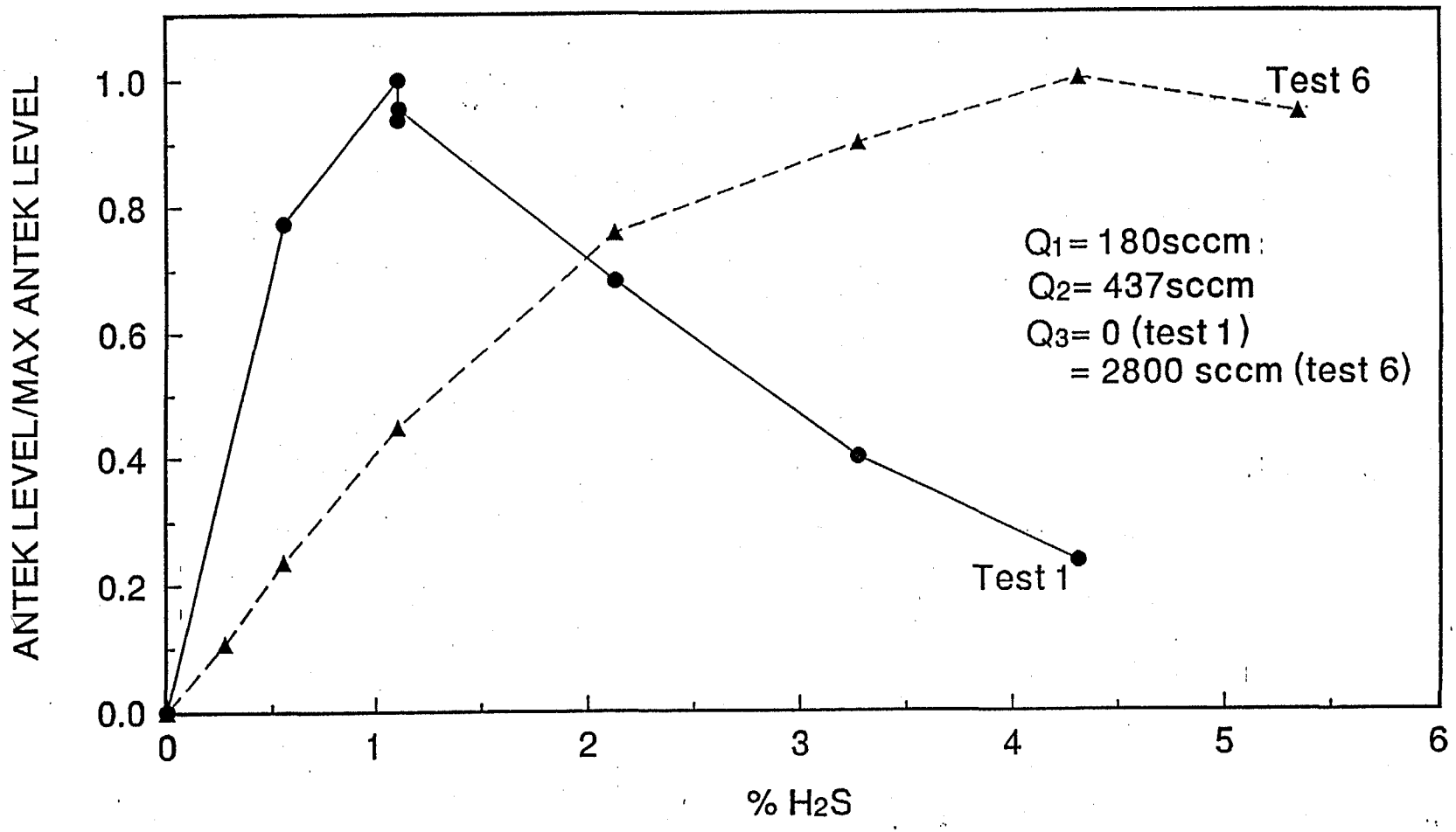

Figure 3. Comparison of High Pressure Calibration Results With and Without Nitrogen Dilution

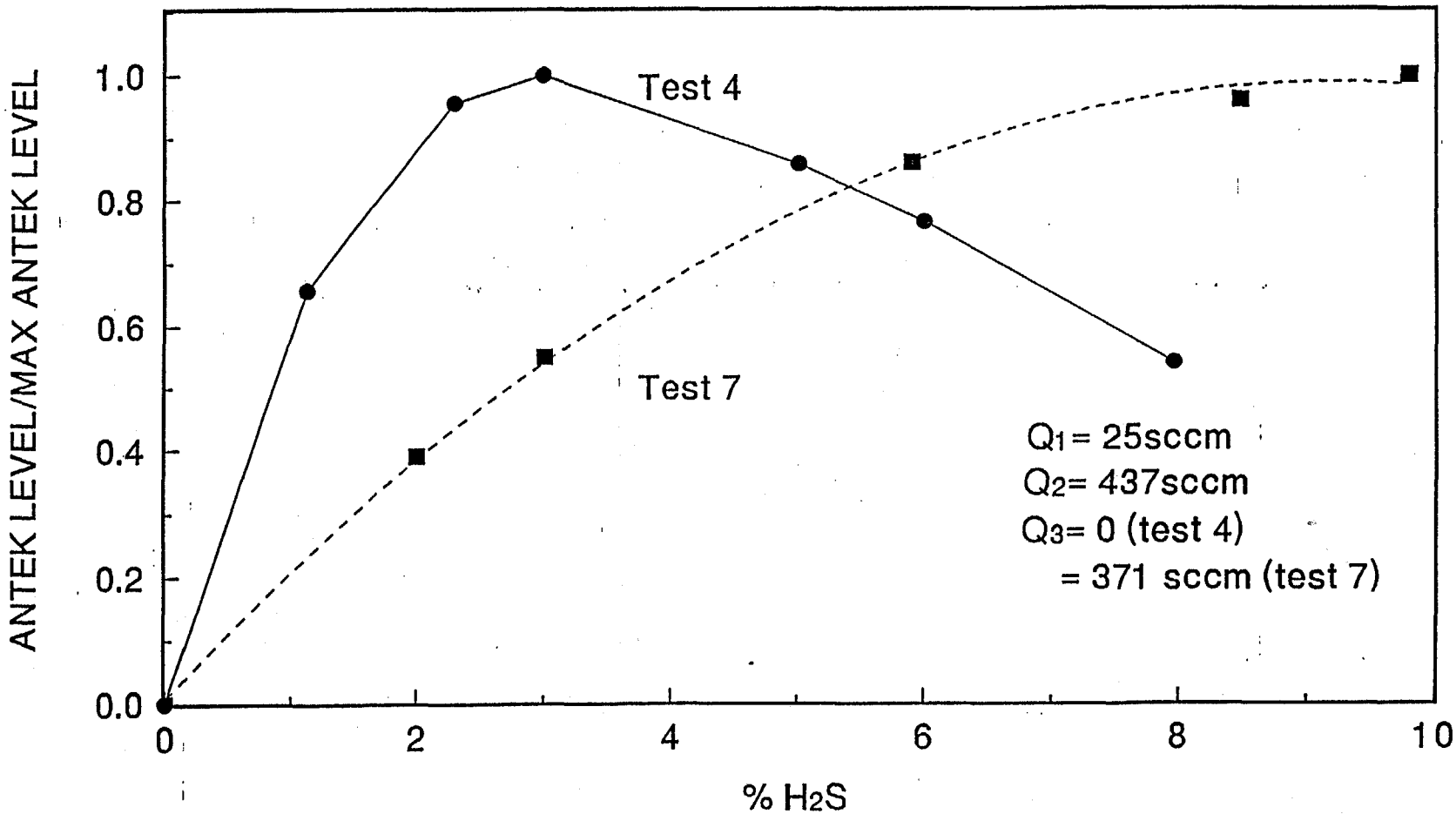

Figure 4. Comparison of Low Pressure Calibration Results With and Without Nitrogen Dilution

An empty reactor was subsequently added to test the reactor system response to varying inlet H_2S concentrations. The reactor was at 50 psig pressure and contained no sorbent for this initial test. Oxygen flow to the pyrotube and diluent N_2 flow downstream of the pyrotube were controlled at 437 sccm and 371 sccm, respectively, as previously discussed. Feed gas containing N_2 and up to 2% H_2S, as determined by mass flow controller settings, was added to the reactor.

Figure 5 compares the Antek response to step function changes in the feed composition as a function of time. The qualitative response was as expected. Except at the beginning, the Antek unit began to sense a composition change after about 2 to 3 minutes. The Antek reading then increased and asymptotically approached a steady state between 5 and 15 minutes later, depending on the total flow rate through the reactor. The initial response was slower because of the start-up procedure employed. Figure 6 is a blow-up of a portion of Figure 5 to show more detail in the Antek response to one of the step function feed concentration changes.

While the qualitative response was as expected, the steady-state Antek concentration levels during the period of H_2S concentration increase were somewhat lower than the levels established by the mass flow controllers and were somewhat higher than the mass flow controller settings during the period of composition decrease. There are a number of possible reasons for these differences which are now being investigated.

First, the test 7 calibration results were established using H_2S concentrations which were generally larger than those used in the Figure 6 response test. The minimum H_2S content used in the calibration test was 2%, while H_2S contents of 0.5, 1.0, and 1.5% were used in the response test. The inclusion of lower H_2S concentrations in the calibration might alter the calibration equation and provide better agreement.

The second source of the problem may be associated with the temperature controller on the photomultiplier tube (PMT) of the UV detector. The PMT temperature should remain constant, but, as shown in Figure 7, a gradual increase in temperature with time was observed. Over the 4 hour duration of test 02, the PMT temperature increased from 10.5°C to 11.2°C. While Antek assures us that this temperature variation is not important at the high concentration levels of this study, they have agreed to repair or replace the temperature controller.

Finally, a third potential cause of the problem could be adsorption/desorption of H_2S on the walls of the reactor and other system components. Adsorption during the period of increasing H_2S concentration would decrease the H_2S concentration reaching the Antek while desorption during the period of decreasing H_2S concentration would increase the concentration to the Antek. If physical adsorption/desorption is the cause of the problem, the effect will be reduced at the higher temperatures to be used for reaction.

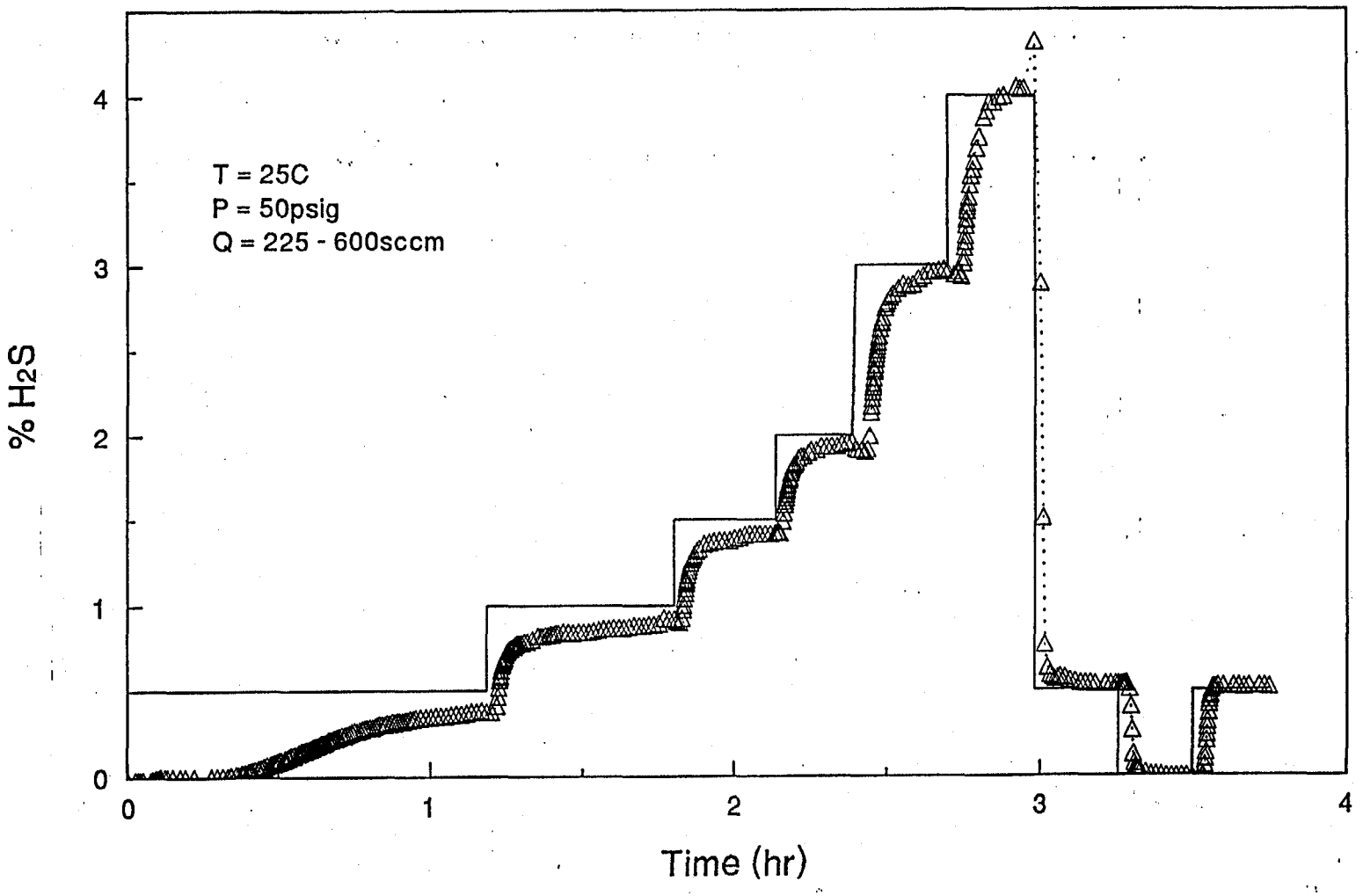

Figure 5. Response of the Antek Total Sulfur Analyzer to Step Function Changes in the H_2S Content of the Feed Gas

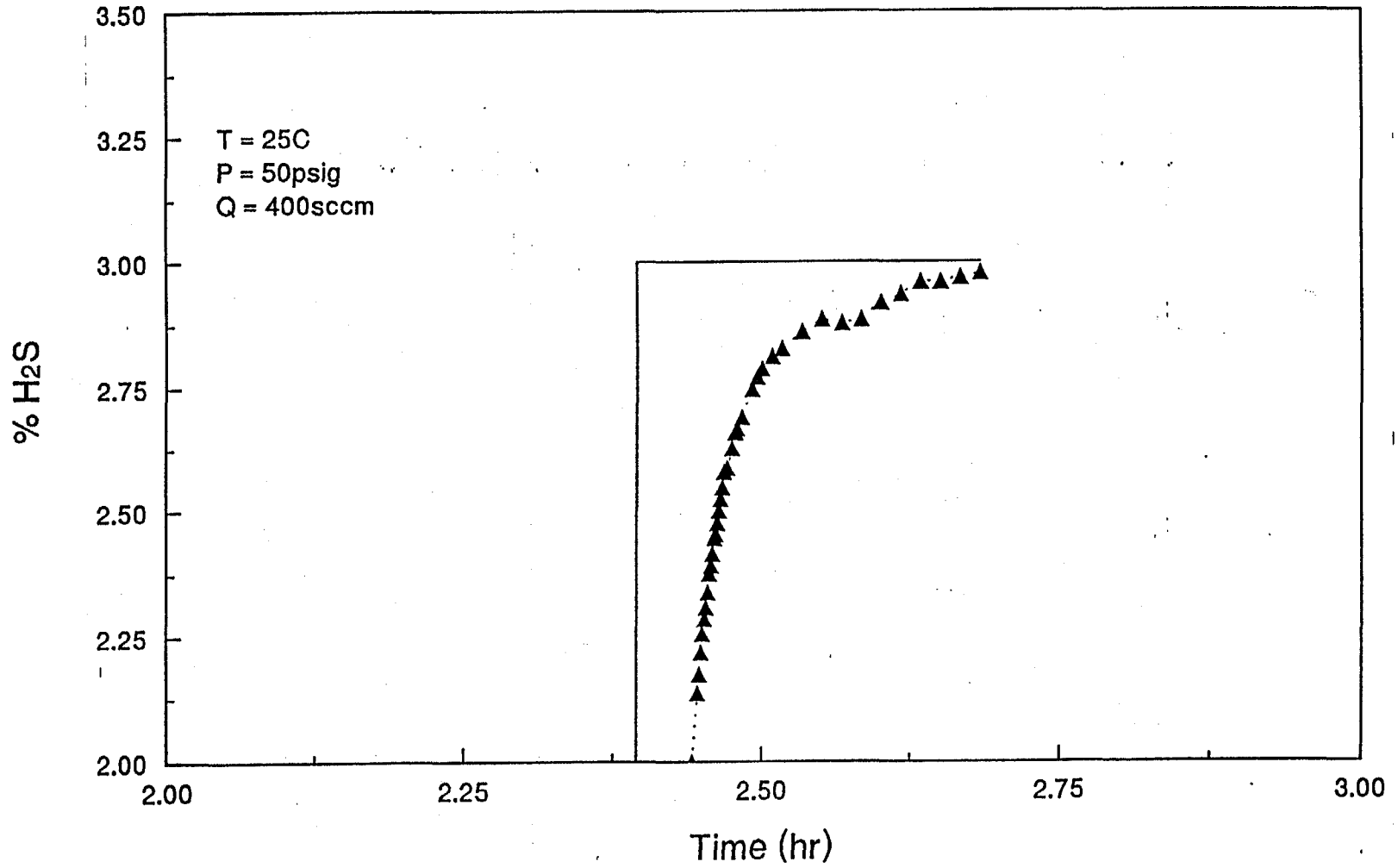

Figure 6. Expanded View of the Antek Response to a Step Function Change in H_2S Content from 2% to 3% (mol %)

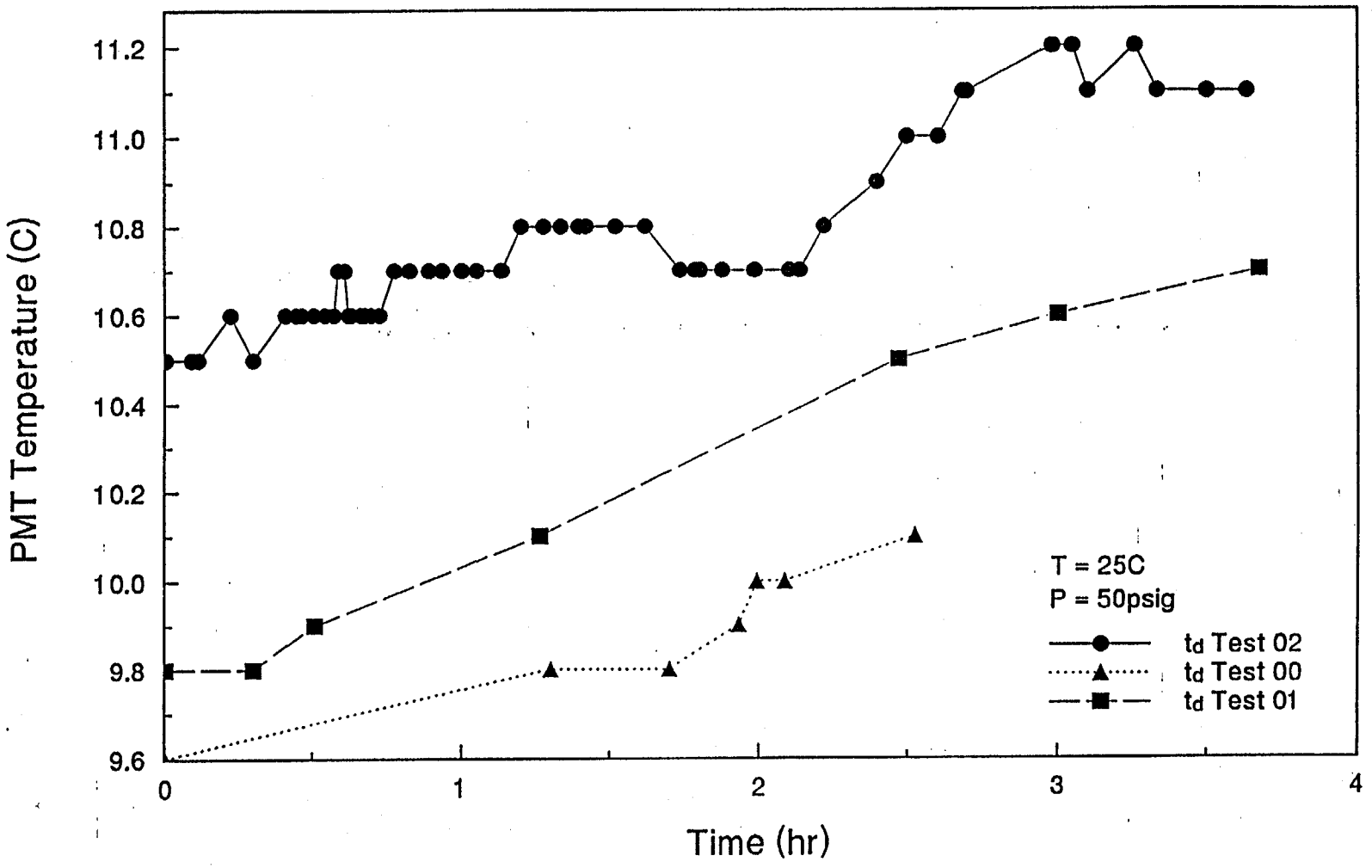

Figure 7. Increase in the Photomultiplier Temperature with Time

ATMOSPHERIC PRESSURE ELECTROBALANCE

Most of the planned experimental program relating to the regeneration of FeS was completed during the quarter. This program examined the effects of volumetric flow rate, temperature, and reactive gas mol fraction on the regeneration reaction in atmospheres of O_2/N_2, H_2O/N_2, and $O_2/H_2O/N_2$. Tables I, II, and III summarize operating conditions and present key results for all tests. Tests completed during the quarter are marked with the asterisk in the first column.

Early tests examined the effect of volumetric flow rate on the reaction rate with the intent of identifying a flow rate above which the reaction rate did not change and mass transfer resistance could be neglected. As a consequence, most of the tests identified in Tables I through III utilized a total gas feed rate of 300 sccm.

The effects of temperature and mol fraction reactive gas on the initial reaction rate are shown in Figures 8 and 9, for the O_2/N_2 and H_2O/N_2 atmospheres, respectively. The straight lines in these figures were determined by linear regression through the origin. More complete statistical analysis of selected data follows. These figures illustrate three important features of the regeneration reactions. First, the initial rate is first-order with respect to both O_2 and H_2O. Secondly, the rate with O_2 is much faster than the rate with H_2O. O_2 mol fractions were varied between 0.005 and 0.03 while H_2O mol fractions were varied between 0.1 and 0.5. The scale of the rate axis extends to 0.06 min^{-1} for O_2 and only to 0.018 min^{-1} for H_2O. Thirdly, over the temperature range of 600°C to 800°C, the effect of temperature on both reactions was quite small.

The series of tests involving regeneration in $O_2/H_2O/N_2$ (Table III) was carried out to determine if the individual reactions proceeded independently, i.e., if the combined rate was equal to the sum of the individual rates. The H_2O mol fraction was held constant at 0.4 in all tests while the O_2 mol fraction was varied between 0.0036 and 0.01. The standard temperature range of 600 to 800°C was covered. The combination of 0.0036 mol fraction O_2 and 0.40 mol fraction H_2O at 800°C was specifically chosen since analysis of the individual initial rates at these conditions suggested that the ratio of H_2S to SO_2 in the product gas should be approximately 2 to 1, which is the ratio associated with the Claus reaction.

Figure 10 summarizes results of the $O_2/H_2O/N_2$ tests in a plot of initial rate versus O_2 mol fraction. The lines at the three temperatures are not fit to the data, but are the predicted rates obtained by summing the single component O_2 and H_2O regeneration rates. The close agreement between predicted and measured rates indicates that, at least initially, the combined reaction rate is given by the sum of the individual rates.

During the regeneration of FeS with O_2 effectively all of the sulfur should be liberated as SO_2. Regeneration with H_2O should liberate sulfur as H_2S. One of the ultimate objectives of the program is to determine if significant quantities of elemental sulfur, S_x, can be formed when the regeneration gas contains both O_2 and H_2O. Because analysis of the effluent gas from

Table I. Operating Conditions and Key Results for the Atmospheric Pressure Electrobalance Tests Involving the Regeneration of FeS in O_2/N_2

	Date	RUN	T	Qt	O2	Mo	M1	M2	(M1/Mo)	(M2/Mo)	rate	K
			C	sccm	%	(mg)	(mg)	(mg)			(min^-1)	(min^-1)
	28/6/95	B6	600	130	0.5	2.688		2.401		0.8935	0.006986	1.397273
	28/6/95	B7	600	130	1	2.729		2.426		0.8891	0.010777	1.077671
	30/6/95	B10	600	130	3	2.6		2.316		0.891	0.033689	1.122969
	30/6/95	B11	600	130	3	2.55		2.27		0.8904	0.03618	1.205997
	05/7/95	C2	600	260	3	2.353		2.098		0.8914	0.043963	1.465445
	07/7/95	C4	600	260	0.5	2.497		2.223		0.8902	0.007226	1.445175
	07/7/95	C5	600	260	1	2.577		2.285		0.8866	0.015205	1.520507
	10/7/95	C6	600	260	1	2.629		2.339		0.8896	0.013538	1.353761
	12/7/95	D2	600	500	1	2.573		2.344		0.9112	0.015467	1.546712
	13/7/95	D3	600	500	3	2.612		2.328		0.8913	0.045763	1.525436
	14/7/95	D4	600	500	0.5	2.671		2.356		0.8823	0.007523	1.504608
	17/7/95	E1	600	300	3	2.693		2.401		0.8918	0.033125	1.104168
	18/7/95	E2	650	300	3	2.439		2.165		0.8877	0.03861	1.28699
	19/7/95	E3	700	300	3	2.622		2.331		0.889	0.049624	1.654137
	20/7/95	E4	600	300	1	2.536		2.261		0.8917	0.011584	1.158387
	24/7/95	E6	600	300	0.5	2.614		2.326		0.8901	0.007715	1.543088
	25/7/95	E7	600	300	1	2.671		2.369		0.8871	0.011423	1.142273
	26/7/95	E8	700	300	0.5	2.486		2.217		0.892	0.007692	1.538347
*	26/10/95	O1	700	300	1	2.366		2.126		0.8986	0.016905	1.690453
*	27/10/95	O2	800	300	1	2.319		2.089		0.9008	0.019254	1.925448
*	27/10/95	O3	800	300	3	2.374		2.144		0.9031	0.052663	1.755443
*	28/10/95	O4	800	300	2	2.344		2.119		0.904	0.038521	1.926074
*	31/10/95	O6	600	300	3	2.346		2.096		0.8935	0.040486	1.349534
*	31/10/95	O7	600	300	2	2.546		2.271		0.892	0.027489	1.374441
*	03/11/95	O8	600	300	1	2.551		2.266		0.8883	0.013632	1.363228
*	03/11/95	O9	600	300	3	2.416		2.156		0.8924	0.038426	1.280882
*	06/11/95	O10	600	300	3	2.456		2.196		0.8942	0.038164	1.272141
*	06/11/95	O11	600	300	3	2.491		2.221		0.8916	0.038225	1.274179

Table II. Operating Conditions and Key Results for the Atmospheric Pressure Electrobalance Tests Involving the Regeneration of FeS in H_2O/N_2

	Date	RUN	T	Qt	H2O	Mo	M1	M2	(M1/Mo)	(M2/Mo)	rate
			C	sccm	%	(mg)	(mg)	(mg)			(min^-1)
	21/8/95	H2	800	286.4	0.162	2.374	2.069	2.159	0.872	0.9094	0.006507
	22/8/95	H3	800	286.4	0.162	2.339	2.039	2.109	0.872	0.9017	0.006109
	23/8/95	H4	800	343.6	0.162	2.426	2.146	2.206	0.885	0.9093	0.005995
	24/8/95	H5	800	343.6	0.162	2.476	2.146	2.226	0.867	0.899	0.006303
	25/8/95	H6	800	335.6	0.249	2.347	2.032	2.122	0.866	0.9041	0.009202
	20/9/95	H14	800	300	0.2	2.47	2.172	2.259	0.879	0.9146	0.008314
	21/9/95	H15	800	300	0.2	2.379	2.08	2.17	0.874	0.9123	0.008388
	23/9/95	H16	800	300	0.4	2.431	2.132	2.171	0.877	0.893	0.013353
*	02/10/95	H18	800	300	0.5	2.329	2.039	-	0.875	-	0.01546
*	03/10/95	H19	700	300	0.424	2.481	2.166	-	0.873	-	0.008061
*	03/10/95	H20	700	300	0.424	2.476	2.146	2.166	0.867	0.8748	0.009872
*	04/10/95	H21	700	300	0.4	2.426	2.081	2.131	0.858	0.8784	0.007556
*	05/10/95	H22	600	300	0.4	2.393	2.071	2.081	0.865	0.8696	0.004634
*	06/10/95	H23	700	300	0.3	2.392	2.093	2.166	0.875	0.9055	0.005992
*	09/10/95	H23	700	300	0.2	2.372	2.066	2.152	0.871	0.9073	0.005177
*	10/10/95	H25	700	300	0.1	2.383	2.066	2.156	0.867	0.9048	0.002343
*	10/10/95	H26	700	300	0.2	2.41	2.086	2.176	0.866	0.9029	0.003993
*	11/10/95	H27	600	300	0.3	2.436	2.121	2.211	0.871	0.9077	0.003323
*	11/10/95	H28	600	300	0.2	2.486	2.158	2.129	0.868	0.8564	0.002164
*	12/10/95	H29	600	300	0.1	2.589	2.261	2.351	0.873	0.9081	0.001159
*	16/10/95	H32	800	300	0.4	2.314	2.029	2.079	0.877	0.8984	0.013507
*	20/10/95	H35	700	300	0.2	2.366	2.096	-	0.886	-	0.007513
*	23/10/95	H38	800	300	0.4	2.369	2.054	-	0.867	-	0.014073
*	24/10/95	H39	800	300	0.4	2.209	1.919	-	0.869	-	0.014489
*	25/10/95	H40	800	300	0.4	2.439	2.099	-	0.861	-	0.014646

Table III. Operating Conditions and Key Results for the Atmospheric Pressure Electrobalance Tests Involving the Regeneration of FeS in $O_2/H_2O/N_2$

	Date	RUN	T	Qt	H2O	O2	Mo	M1	M2	(M1/Mo)	(M2/Mo)	rate
			C	sccm	%	%	(mg)	(mg)	(mg)			(min^-1)
*	07/11/95	P1	800	300	40	0.36	2.444	2.169	2.189	0.887	0.8956	0.089108
*	08/11/95	P2	800	300	40	1	2.399	2.149	2.159	0.896	0.8999	0.039375
*	09/11/95	P3	800	300	40	1	2.409	2.169	2.179	0.9	0.9045	0.034599
*	09/11/95	P4	800	300	40	0.36	2.219	2.004	2.009	0.903	0.9053	0.019317
*	16/11/95	P5	800	300	40	0.7	2.519	2.279	2.294	0.905	0.9107	0.02647
*	16/11/95	P6	700	300	40	0.7	2.461	2.236	2.241	0.909	0.9106	0.020315
*	17/11/95	P7	700	300	40	1	2.421	2.196	2.196	0.907	0.9071	0.023404
*	20/11/95	P8	700	300	40	0.36	2.36	2.136	2.166	0.905	0.9178	0.014251
*	21/11/95	P9	600	300	40	0.36	2.461	2.221	2.221	0.902	0.9025	0.009141
*	21/11/95	P10	600	300	40	0.7	2.411	2.171	2.221	0.9	0.9212	0.013095
*	22/11/95	P11	600	300	40	1	2.396	2.171	2.221	0.906	0.927	0.01707

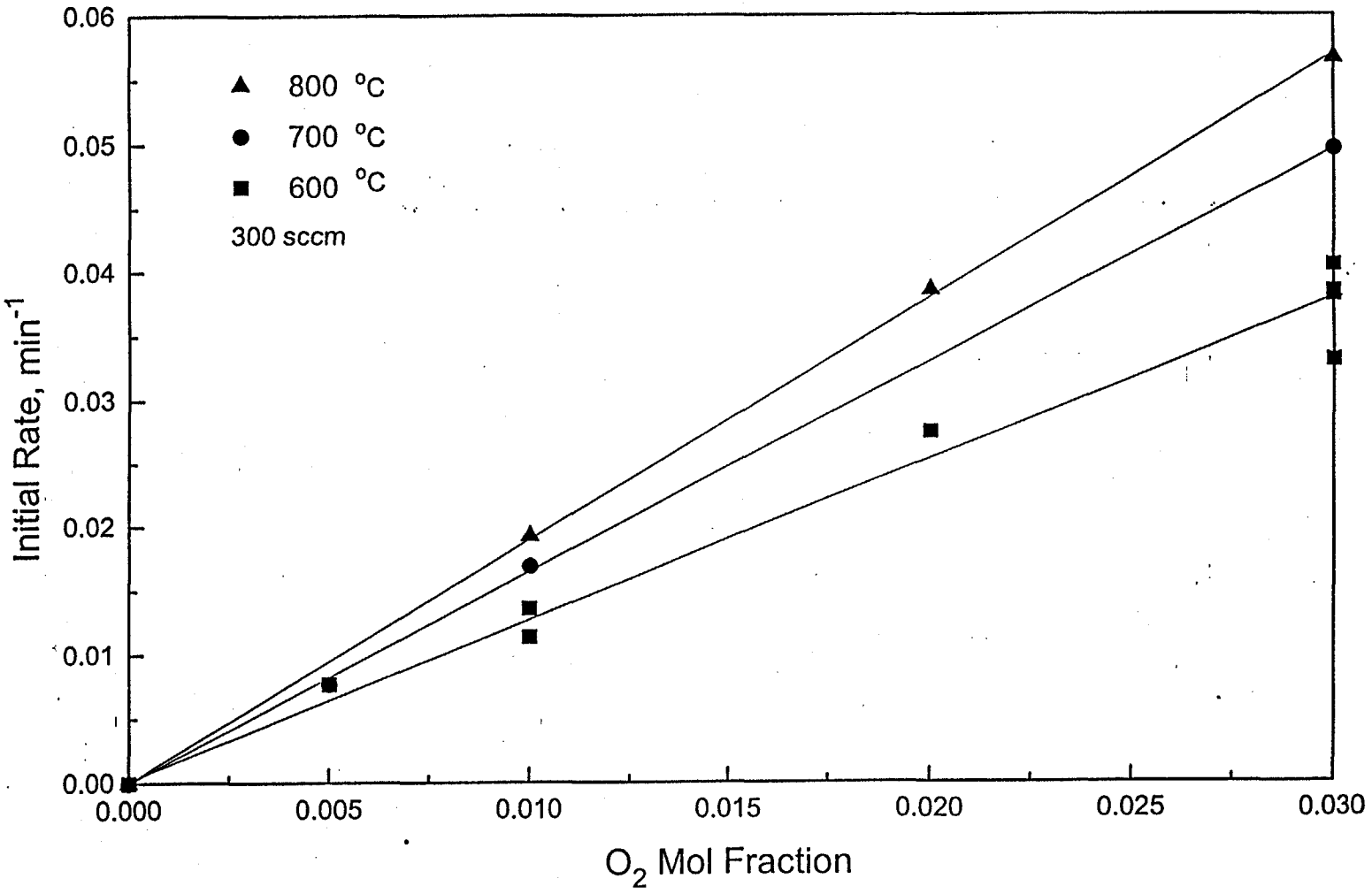

Figure 8. The Effect of Temperature and O_2 Mol Fraction on the Initial Regeneration Rate of FeS

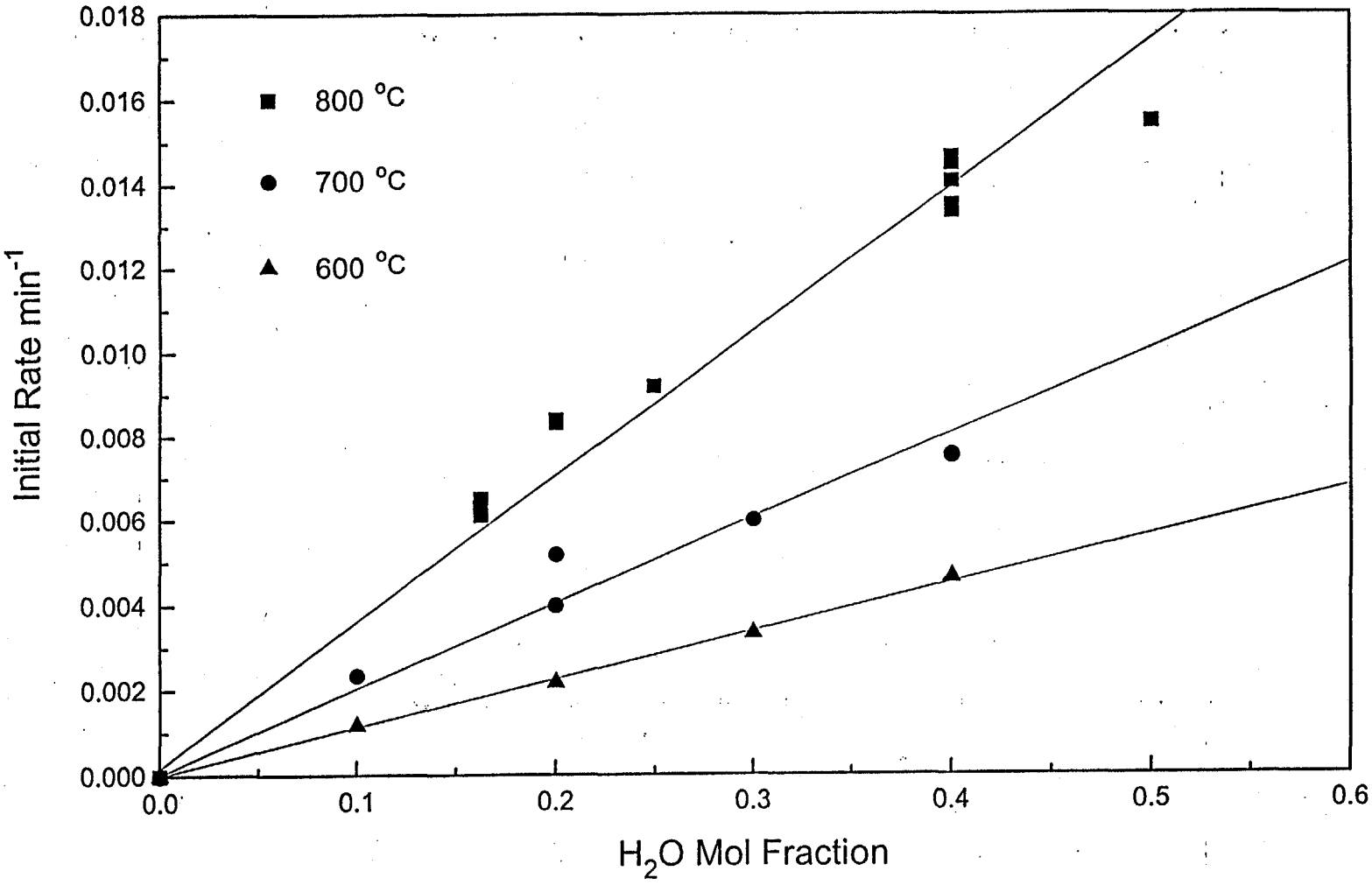

Figure 9. The Effect of Temperature and H_2O Mol Fraction on the Initial Regeneration Rate of FeS

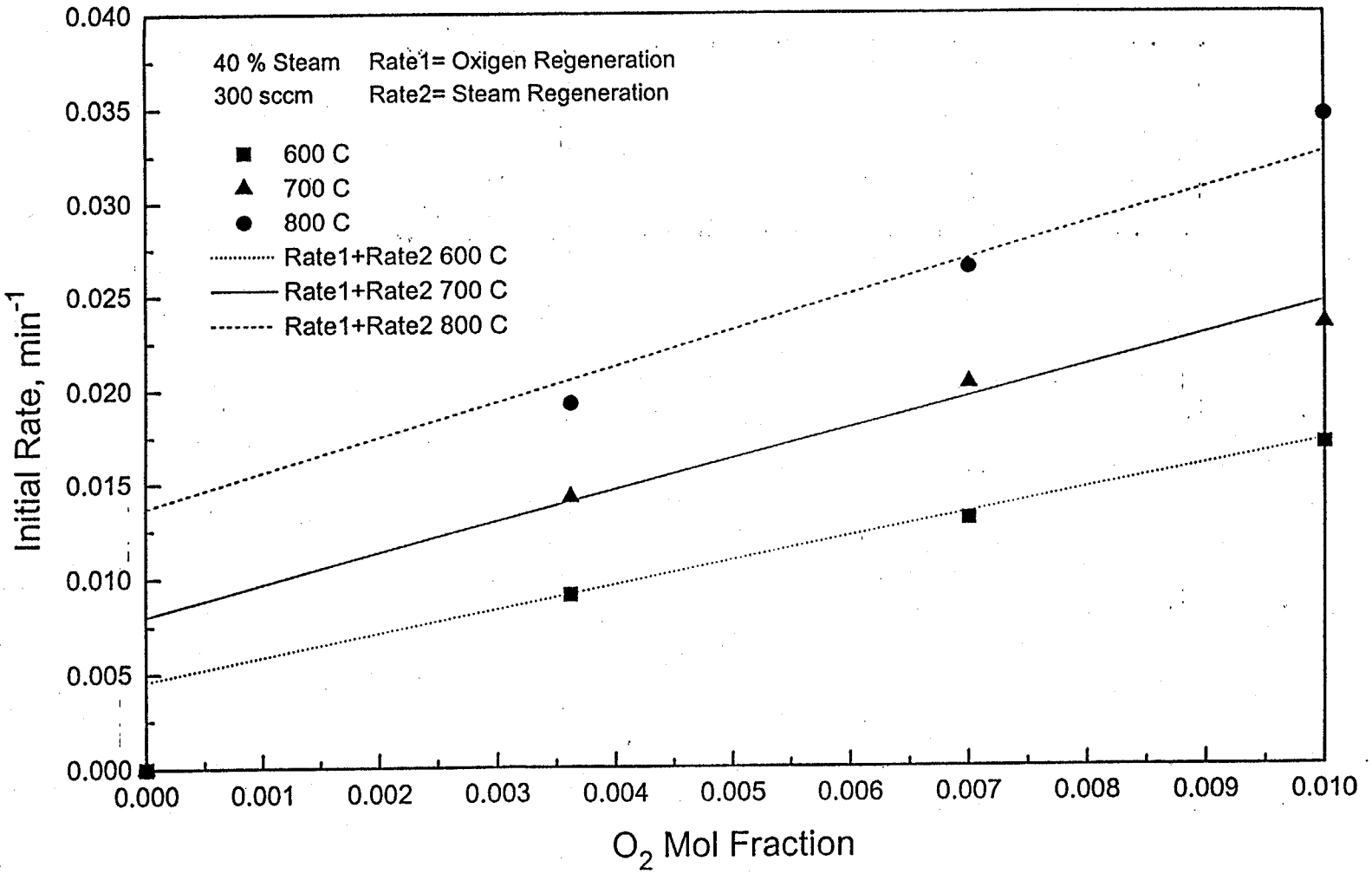

Figure 10. Initial Regeneration Rate of FeS in an $O_2/H_2O/N_2$ Atmosphere: Comparison with Pure Component Rates

the electrobalance was not possible, the only way to determine if elemental sulfur was formed would be visually. No sulfur was observed in the above tests. This was not surprising, however, as only about 0.8 mg of sulfur could be formed if all sulfur in a 2.3 mg sample of FeS was liberated in elemental form. Hence, one test was conducted in which the initial FeS sample size was increased to 50 mg, thus increasing the potential elemental sulfur yield to 18 mg. A yellow deposit was formed near the exit of the quartz hangdown tube. Although it was not possible to estimate the amount, this deposit provided definite proof that some elemental sulfur was formed.

Five duplicate tests were performed at two sets of conditions to provide information of the reproducibility of the initial rate measurements. Results are shown in Figure 8 for the five O_2/N_2 tests at 600°C using 3% O_2, in Figure 9 for the five H_2O/N_2 tests at 800°C using 40% H_2O, and are presented in greater detail in Table IV. The range in initial rates for the O_2/N_2 duplicate tests was from 0.0331 min^{-1} to 0.0405 min^{-1} with mean plus/minus standard deviation values of 0.0377 $\pm$ 0.0027 min^{-1}. For the H_2O/N_2 duplicate tests the range was from 0.0133 to 0.0146 min^{-1} with mean plus/minus standard deviation of 0.0140 $\pm$ 0.006 min^{-1}.

Figure 11 shows the results of a statistical analysis of the effect of O_2 mol fraction on the initial regeneration rate at 600°C. Results of 10 tests, including the five duplicates at 0.03 O_2 and three duplicates at 0.01 O_2, are included. Single tests were conducted at 0.005 O_2 and 0.02 O_2. The solid straight line represents the best-fit through the origin while the dashed straight line represents the best unconstrained linear fit. The two curved dashed lines represent the 95% confidence limits based on the unconstrained straight line. The two straight lines are, for practical purposes, identical, with the intercept of the unconstrained line being only 0.0012. The slope of the lines, which is proportional to the reaction rate constant, is 1.287 min^{-1} for the constrained best-fit, and 1.219 min^{-1} for the unconstrained best fit. Results from 9 of the 10 tests lie within the 95% confidence limits.

Similar analysis for the regeneration in H_2O/N_2 is presented in Figure 12. Regeneration conditions were 800°C with the H_2O mol fraction ranging between 0.15 and 0.50. Results from twelve tests are included with duplicate tests at 0.15 O_2 and 0.40 O_2. In this case there is a larger difference between the constrained and unconstrained straight lines, with the latter having an intercept of 0.002. The slopes are 0.0359 for the constrained line through the origin and 0.0293 for the unconstrained line. Only one of the test results falls outside the 95% confidence limits.

Finally, Figure 13 shows comparable results for a limited test series for O_2 regeneration at 800°C where only three tests were carried out. Once again, the constrained and unconstrained best-fit lines are effectively equal. Although all three data points are very near the unconstrained line, the spread in the 95% confidence limits is larger because of the small number of data points.

The relatively small effect of temperature on the initial reaction rate is emphasized in Figure 14, which presents Arrhenius plots of the rate constant for both O_2 and H_2O regeneration

Table IV. Initial Rate Measurements from Multiple Tests at the Same Reaction Conditions

Regeneration of FeS in O_2/N_2 : T=600°C, 3% O_2

Test No.	Initial Rate, min^{-1}
O11	0.0382
O10	0.0381
O09	0.0384
O06	0.0405
E01	0.0331
Mean ± Std. Dev.	0.037 ± 0.0027

Regeneration of FeS in H_2O/N_2 : T=800°C, 40% H_2O

Test No.	Initial Rate, min^{-1}
H16	0.0133
H32	0.0135
H38	0.0141
H39	0.0145
H40	0.0146
Mean ± Std. Dev.	0.0140 ± 0.006

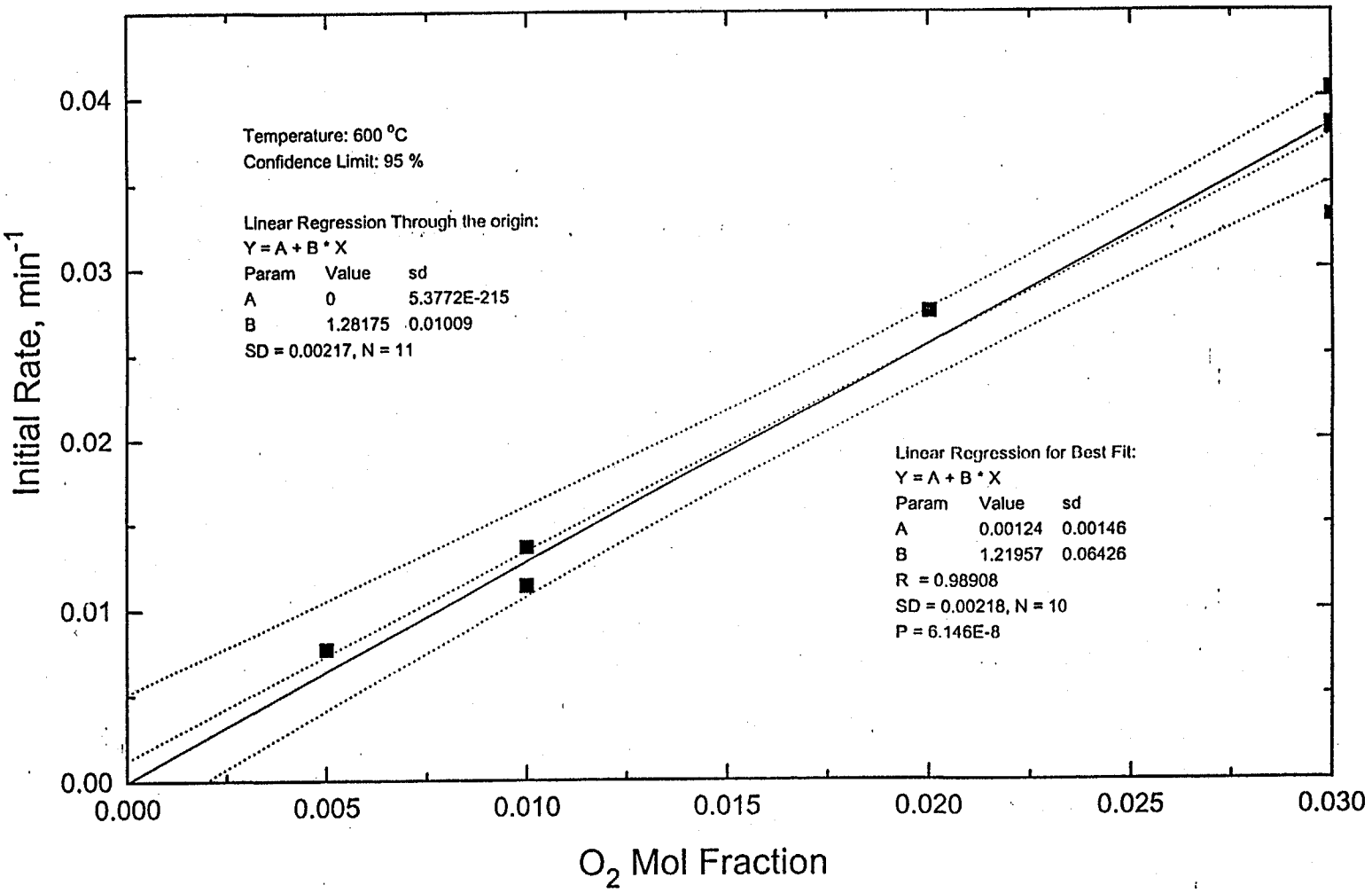

Figure 11. Statistical Analysis of the Initial Regeneration Rate of FeS in O_2/N_2 in the Atmospheric Pressure Electrobalance: T=600°C

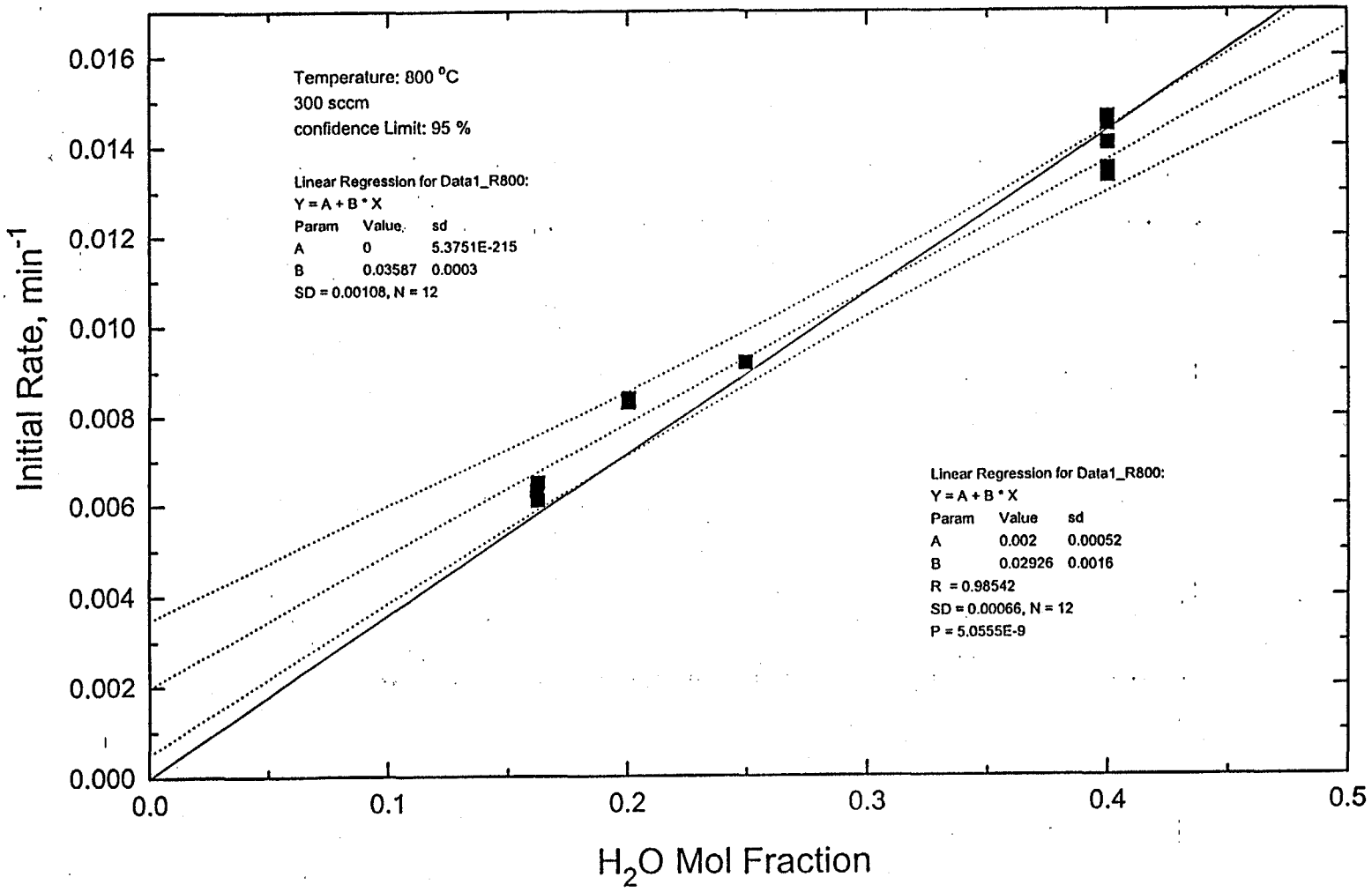

Figure 12. Statistical Analysis of the Initial Regeneration Rate of FeS in H_2O/N_2 in the Atmospheric Pressure Electrobalance: T=800°C

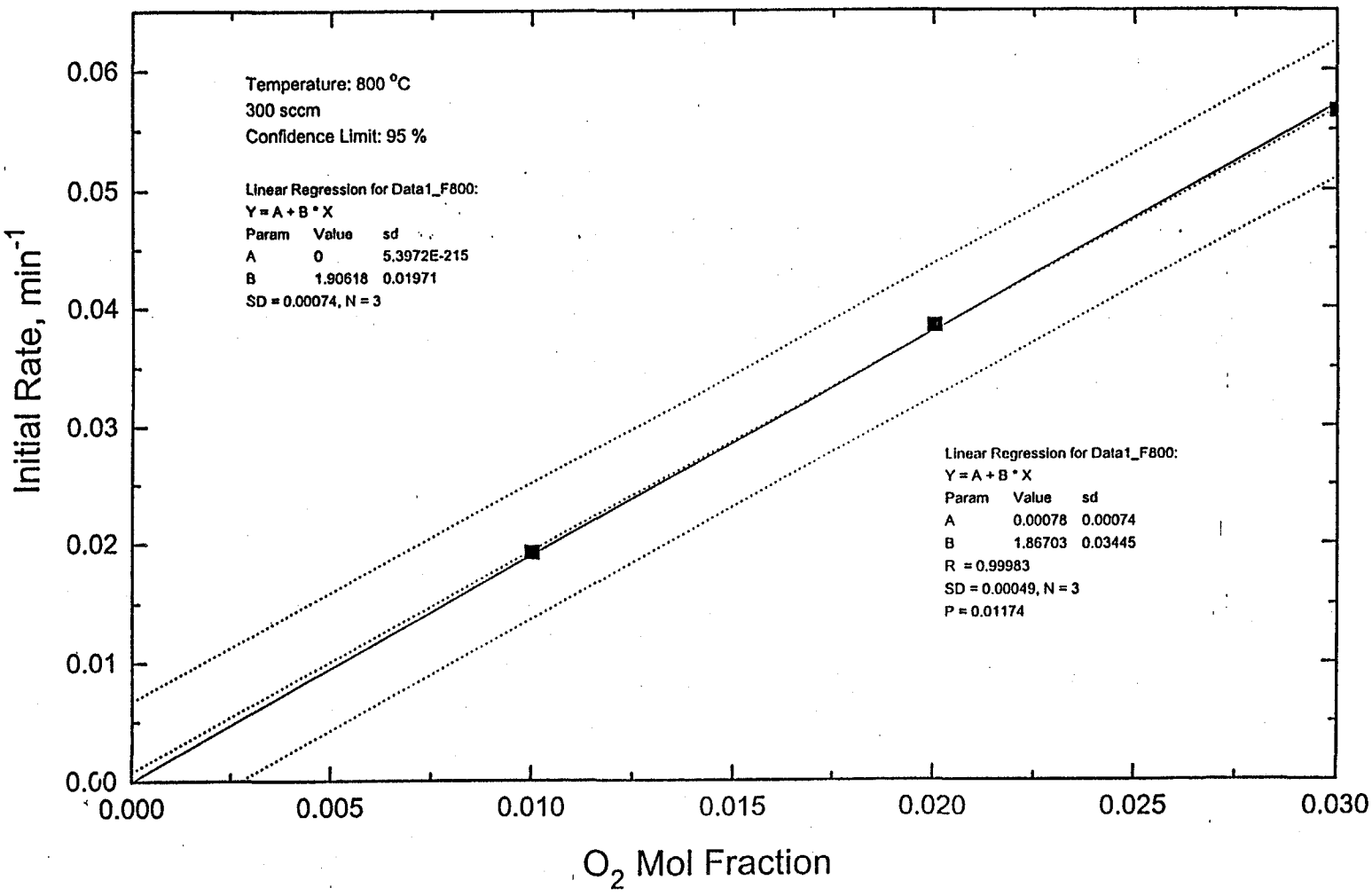

Figure 13. Statistical Analysis of Limited Data on the Initial Regeneration Rate of FeS in O_2/N_2 in the Atmospheric Pressure Electrobalance: T=800°C

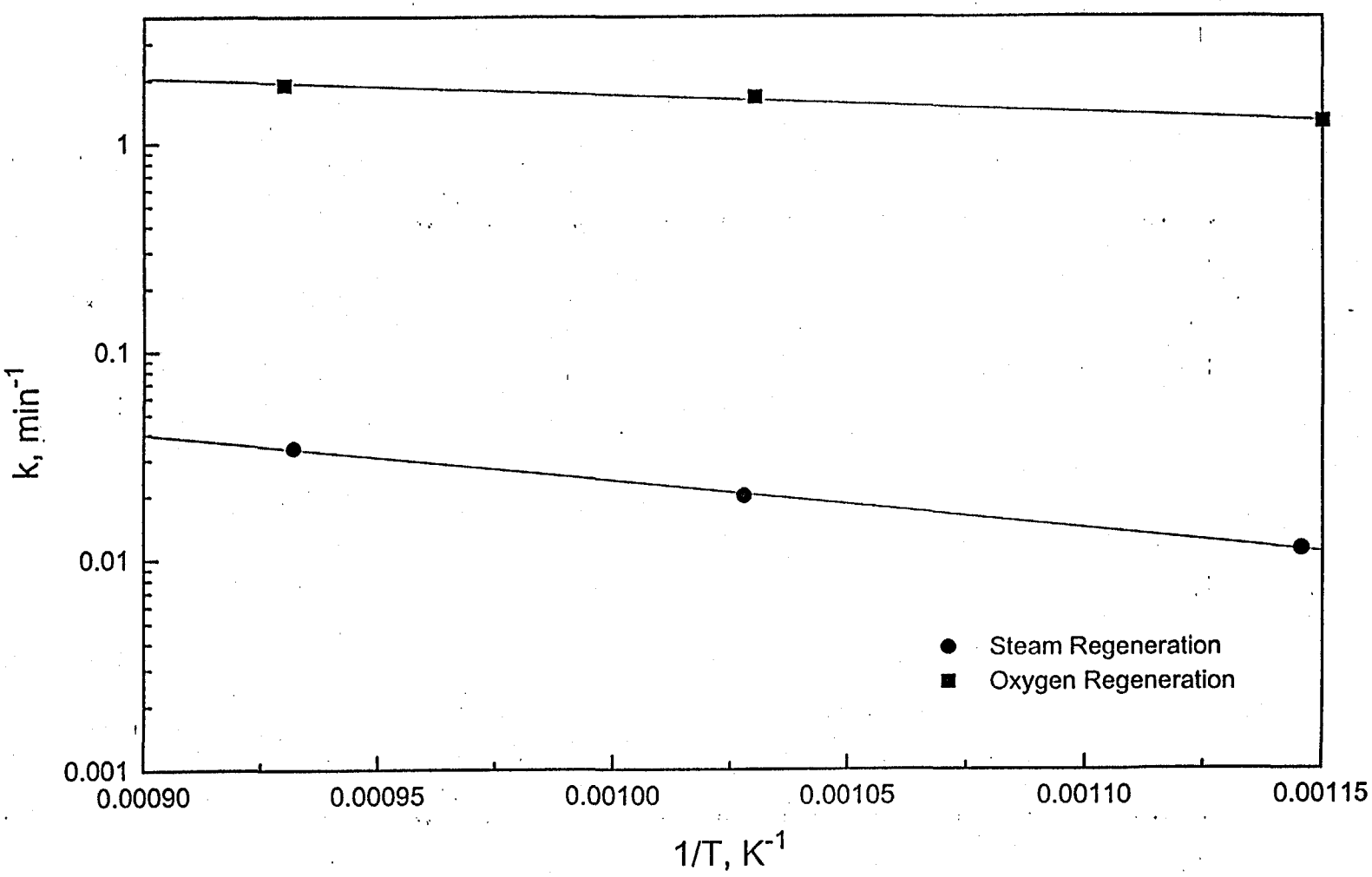

Figure 14. Arrhenius Plot for the Regeneration of FeS in O_2/N_2 and H_2O/H_2 in the Atmospheric Pressure Electrobalance

versus the inverse of the absolute temperature. The data points are the slopes of the best-fit lines through the origin from Figures 8 and 9. The slopes of the best-fit Arrhenius lines are -1892 and -5175 for O_2 and H_2O, respectively. From this analysis, the rate equations, based on initial rates, for the regeneration of FeS can be written as

$$r_{O_2} = 11.2\ e^{-3760/RT}\ y_{O_2} \qquad \text{in oxygen}$$

$$r_{H_2O} = 4.2\ e^{-10,280/RT}\ y_{H_2O} \qquad \text{in steam}$$

r has units of min^{-1}, T is the absolute temperature, R is the gas constant, and y is the mol fraction of either oxygen or steam. At 800°C and equal mol fractions, the regeneration rate in O_2 is about 56 times larger than the regeneration rate in H_2O.

HIGH PRESSURE ELECTROBALANCE

The FeS regeneration test series in H_2O was completed during the quarter. We had thought that the O_2 regeneration series was also complete, although further analysis of the data has indicated the need for additional tests to reduce the data scatter. Tables V and VI summarize operating conditions and present key results for all O_2 and H_2O regeneration tests, respectively. Those tests completed during the past quarter are marked with an asterisk. The following presentation is limited to the H_2O/N_2 test series because the additional O_2/N_2 runs may alter the results somewhat. Experimental problems associated with steam condensation on cool sections of the hangdown tube were experienced. These problems became more severe as the mol fraction of H_2O and the operating pressure increased. Heat tracing eliminated the condensation problem except at the highest pressure (15 atm) and largest H_2O mol fraction (0.40). As a consequence, 15 atm tests were limited to a maximum H_2O mol fraction of 0.30 compared to the maximum H_2O mol fraction of 0.40 in 1 and 5 atm tests. The temperature range covered was 600°C to 800°C.

Figure 15 shows the effect of H_2O mol fraction and pressure on the initial regeneration rate at a temperature of 700°C. The straight lines corresponding to each pressure were determined by linear regression without the constraint that the line pass through the origin. Each of the lines has a small negative intercept. The most interesting result from this figure is the effect of pressure at constant H_2O mol fraction. The maximum rate corresponded to the intermediate pressure of 5 atm. The rates were intermediate at low pressure (1 atm) and the lowest rates were measured at the maximum pressure (15 atm).

This effect of pressure is emphasized in Figure 16 where the initial regeneration rate at 600°C is plotted versus pressure with H_2O mol fraction as the parameter. The rate increased

Table V. Operating Conditions and Key Results for the High Pressure Electrobalance Tests Involving the Regeneration of FeS in O_2/N_2

Date	Run	T	Qt	O2	P	Mo	M1	M2	M1/Mo	M2/Mo	Rate
		(C)	(sccm)	(%)	(atm)	(mg)	(mg)	(mg)			(min^-1)
7/31/95	F 37	600	800	3	1	2.545		2.311		0.908	0.0400
7/31/95	F 38	600	1000	3	1	2.380		2.161		0.908	0.0483
8/1/95	F 39	800	1000	3	15	2.898		2.631		0.908	0.0350
8/1/95	F 40	800	800	3	15	3.920		3.559		0.908	0.0350
8/15/95	F 42	700	800	3	15	2.540		2.304		0.907	0.0300
8/16/95	F 43	650	800	3	15	3.060		2.739		0.895	0.0125
8/17/95	F 44	625	800	3	15	3.360		3.064		0.912	0.0125
8/17/95	F 45	600	800	3	15	3.048		2.926		0.960	0.0214
8/22/95	F 47	600	800	1	1	2.910		2.619		0.900	0.0100
8/22/95	F 48	700	800	0.5	1	3.470		3.151		0.908	0.0059
8/22/95	F 49	700	800	1	1	3.060		2.754		0.900	0.0114
8/23/95	F 50	700	800	3	1	3.920		3.559		0.908	0.0358
8/24/95	F 51	700	800	0.5	1	2.934		2.655		0.905	0.0060
8/24/95	F 52	600	800	0.5	1	2.900		2.633		0.908	0.0056
8/25/95	F 53	800	800	1	1	2.734		2.485		0.909	0.0150
8/28/95	F 54	600	800	1	5	2.572		2.335		0.908	0.0180
8/28/95	F 55	700	800	0.5	5	2.275		2.052		0.902	0.0067
8/29/95	F 56	700	800	1	5	2.284		2.062		0.903	0.0175
8/29/95	F 57	700	800	3	5	2.117		1.916		0.905	0.0400
8/30/95	F 58	700	800	3	5	3.004		2.704		0.900	0.0400
9/1/95	F 59	800	800	1	5	4.310		3.879		0.900	0.0164
9/5/95	F 60	700	800	0.5	15	3.006		2.705		0.900	0.0067
9/6/95	F 61	700	800	1	15	2.436		2.192		0.900	0.0150
9/6/95	F 62	800	800	0.5	1	3.520		3.168		0.900	0.0082
9/7/95	F 63	800	800	3	1	3.034		2.731		0.900	0.0429
9/7/95	F 64	600	800	0.5	5	4.680		4.212		0.900	0.0092
9/8/95	F 65	600	800	3	5	2.916		2.654		0.910	0.0450
9/8/95	F 66	800	800	0.5	5	4.510		4.104		0.910	0.0078
9/11/95	F 67	800	800	3	5	2.791		2.512		0.900	0.0467
9/11/95	F 68	600	800	0.5	15	2.469		2.247		0.910	0.0045
9/12/95	F 69	600	800	1	15	3.195		2.994		0.937	0.0060
9/13/95	F 70	800	800	0.5	15	3.450		3.105		0.900	0.0054
9/22/95	F 75	600	800	1	1	4.600		4.140		0.900	0.0100
* 10/6/95	F 80	800	800	1	15	2.639		2.401		0.910	0.0220
* 10/9/95	F 81	700	800	0.5	1	3.159		2.859		0.905	0.0072
* 10/9/95	F 82	600	800	3	5	4.340		3.949		0.910	0.0360
* 10/10/95	F 83	800	800	1	15	2.988		2.704		0.905	0.0150
* 10/11/95	F 84	600	800	3	5	2.796		2.533		0.906	0.0400
* 10/12/95	F 85	800	800	1	15	3.157		2.873		0.910	0.0188
* 10/13/95	F 86	700	800	0.5	1	2.527		2.274		0.900	0.0064
* 10/16/95	F 87	700	800	0.5	1	2.775		2.498		0.900	0.0068

Table VI. Operating Conditions and Key Results for the High Pressure Electrobalance Tests Involving the Regeneration of FeS in H_2O/N_2

Date	Run	T	Qt	H2O	P	Mo	M1	M2	(M1/Mo)	(M2/Mo)	Rate
		(C)	(sccm)	(%)	(atm)	(mg)	(mg)	(mg)			(min^-1)
10/12/95	S 02	800	800	10	1	3.093	2.691		0.870		0.0040
10/13/95	S 03	600	800	40	1	3.650	3.176		0.870		0.0045
10/24/95	S 13	600	800	10	1	4.270	3.758		0.880		0.0010
10/26/95	S 15	700	800	10	1	2.775	2.417		0.871		0.0017
10/27/95	S 16	600	800	30	1	2.280	2.006		0.880		0.0033
11/2/95	S 17	700	800	30	1	2.449	2.106		0.860		0.0067
11/6/95	S 19	800	800	30	1	2.776	2.432		0.876		0.0102
11/7/95	S 21	700	800	40	1	3.650	3.212		0.880		0.0080
11/7/95	S 22	800	800	40	1	3.630	3.158		0.870		0.0134
11/14/95	S 27	800	800	30	5	2.930	2.520		0.860		0.0130
11/16/95	S 29	700	800	40	5	2.350	2.045		0.870		0.0140
11/17/95	S 30	800	800	40	5	2.580	2.270		0.880		0.0190
11/27/95	S 36	600	800	10	5	2.682	2.360		0.880		0.0020
11/28/95	S 37	700	800	10	5	2.422	2.131		0.880		0.0030
11/29/95	S 38	800	800	10	5	2.224	1.957		0.880		0.0040
11/30/95	S 39	600	800	40	5	2.983	2.595		0.870		0.0070
12/1/95	S 40	600	800	30	5	2.372	2.087		0.880		0.0055
12/3/95	S 41	700	800	30	5	2.389	2.102		0.880		0.0100
12/7/95	S 45	800	800	10	15	2.651	2.333		0.880		0.0014
12/18/95	S 49	700	800	10	15	2.637	2.321		0.880		0.0012
12/19/95	S 50	600	800	10	15	2.406	2.117		0.880		0.0005
12/21/96	S 53	800	800	30	15	2.788	2.453		0.880		0.0042
12/22/96	S 54	700	800	30	15	2.456	2.161		0.880		0.0038
12/23/96	S 55	600	800	30	15	2.937	2.555		0.870		0.0016
12/25/96	S 57	600	800	20	15	3.100	2.728		0.880		0.0010
12/26/96	S 58	700	800	20	15	2.987	2.629		0.880		0.0025
12/27/96	S 59	800	800	20	15	2.905	2.556		0.880		0.0030

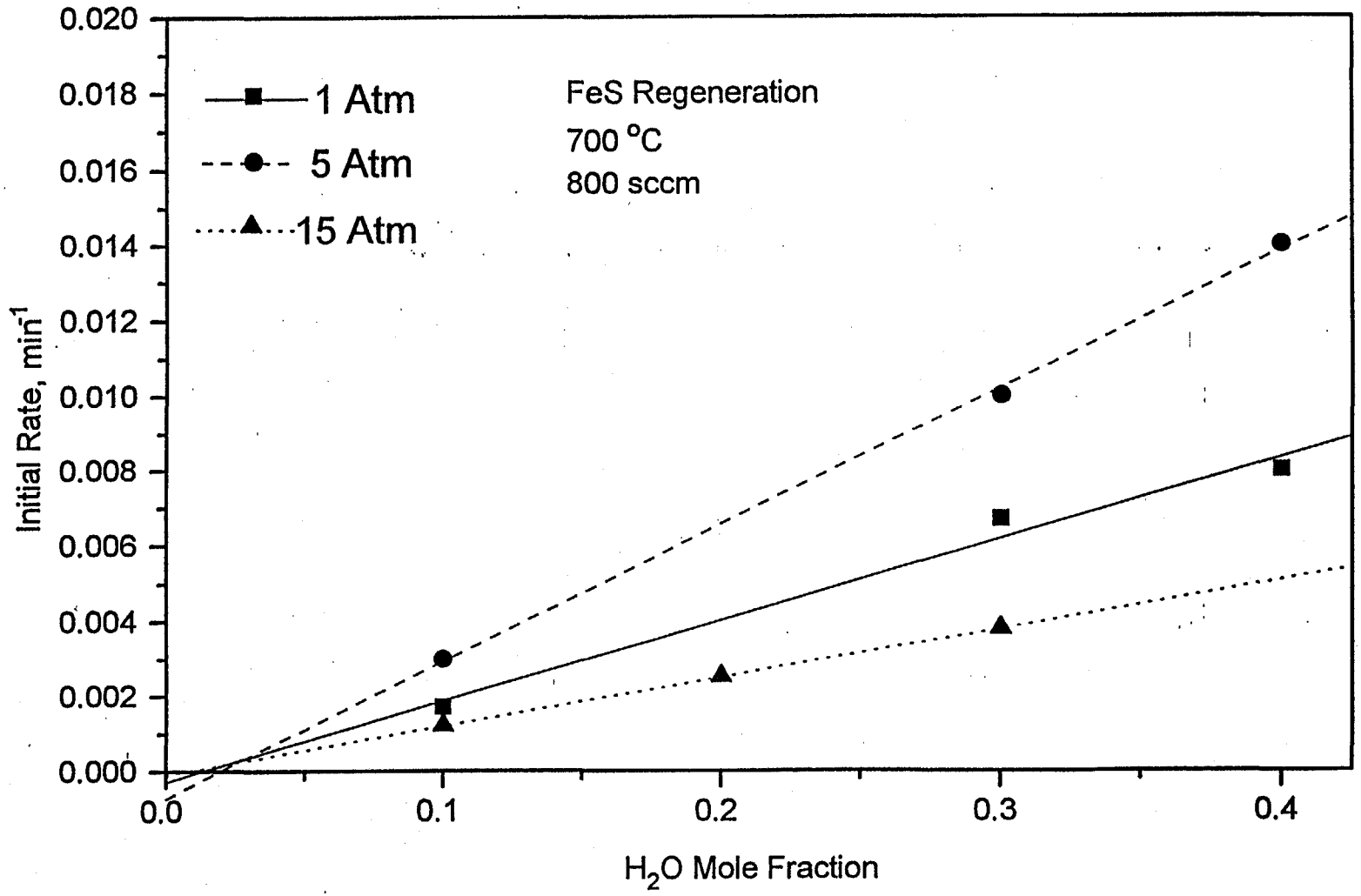

Figure 15. The Effect of H_2O Mol Fraction and Pressure on the Initial Regeneration Rate of FeS: T=700°C

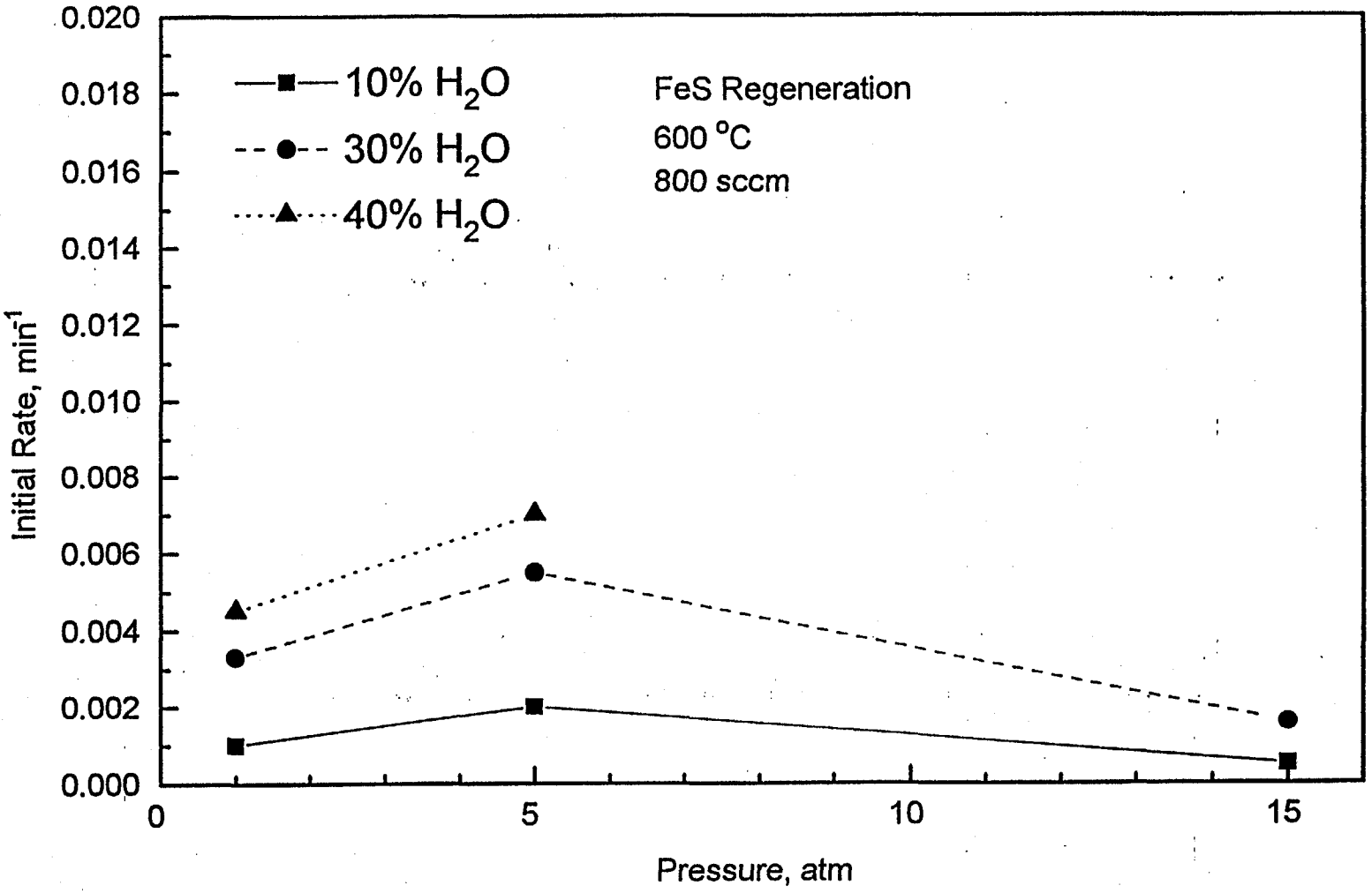

Figure 16. The Effect of pressure and H_2O Mol Fraction of the Initial Regeneration Rate of FeS: T=600°C

as the pressure increased from 1 to 5 atm at each mol fraction, and then the rate decreased for both mol fractions as the pressure was further increased from 5 to 15 atm.

The small effect of temperature which was found for both regeneration reactions using the atmospheric pressure electrobalance was confirmed at the higher pressures. This is illustrated in Figure 17 where the initial rate using 30% H_2O is plotted versus temperature with reaction pressure as the parameter.

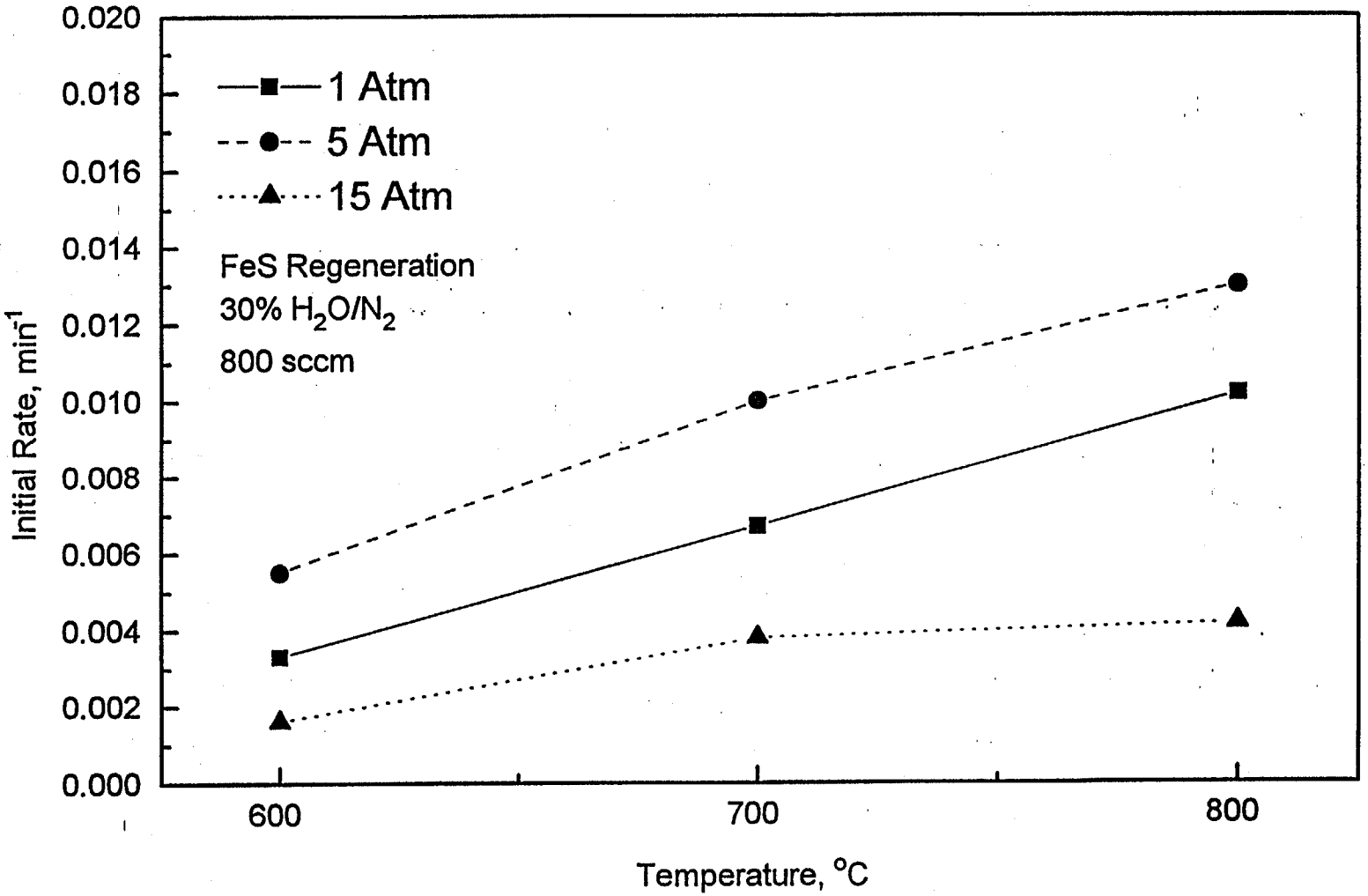

Figure 17. The Effect of Temperature and Pressure on the Initial Regeneration Rate of FeS in 30% H_2O/N_2